Available online at www.sciencedirect.com

SCIENCE DIRECT®

Thermochimica Acta 446 (2006) 36–40

thermochimica acta

www.elsevier.com/locate/tca

4,4′-Azoxyanisole for temperature calibration of differential scanning calorimeters in the cooling mode—Yes or no?

Heiko K. Cammenga[a], Karin Gehrich[a], Stefan M. Sarge[b,*]

[a] Institut für Physikalische Chemie, Technische Universität Braunschweig, Hans-Sommer-Straße 10, 38106 Braunschweig, Germany
[b] Physikalisch-Technische Bundesanstalt, Bundesallee 100, 38116 Braunschweig, Germany

Dedicated to Professor Wolfgang Hemminger on the occasion of his 65th anniversary.

Abstract

By measuring the transition peak using differential scanning calorimetry in the heating and cooling modes, it has been confirmed that the nematic-to-isotropic liquid phase transition of 4,4′-azoxyanisole is of first order, but with some underlying additional phenomenon. As a consequence, this phase transition can only be used under certain precautions for temperature calibration of scanning calorimeters in the cooling mode.

Keywords: Calibration; Temperature calibration; Cooling mode; Differential scanning calorimeter; Liquid crystal; 4,4′-Azoxyanisole

---

1. Introduction

It is generally accepted that when conducting differential scanning calorimetry (DSC) experiments in the cooling mode, for reaching the best possible measurement uncertainty it is advisable to perform the calibration of the instrument also in the cooling mode [1–8]. Liquid crystals have been shown to be interesting for the calibration of DSCs in the cooling mode. It has been stated that some of the transitions within their phase systems are of higher order and are thus not subjected to the phenomenon of supercooling. This is a desirable feature of calibration substances for use on cooling [1,4,8]. The problem is to unequivocally distinguish phase transitions of first order from those of higher order by the methods usually available to thermoanalysts. A further requirement imposed on the combination of instrument and calibration substance is a sufficiently good resolution. This means that in the case where the substance shows two transitions close to each other, the instrument must be able to separate the two peaks completely and to reach the baseline between them [9,10].

Thermodynamic criteria for the supposed order of the transition are the heat capacity, the coefficient of expansion and the compressibility versus temperature functions. 4,4′-Azoxyanisole (cf. Fig. 1) is one of the earliest well-characterised and interpreted liquid crystals with nematic-to-isotropic liquid phase transition [11]. The shape of the curves published show a Lambda-like appearance. The conclusion should be that this phase transition is of higher order. Investigations of this phase transition by DSC [12], however, show a first-order behaviour: By measuring the phase transition peak at different heating rates, the peak height increased by a factor of $\sqrt{2}$ when doubling the heating rate. This is a clear indication of a first-order phase transition, which is accompanied by a phase transition enthalpy. With phase transitions of higher order, this factor should be 2 because without enthalpy change, the apparent heat capacity of a sample should double when doubling the heating rate [13,14]. In contrast to this, the Landau theory yields an order of this transition, which can only be described as “weakly first order” [15, pp. 76–91, 16, 17].

4,4′-Azoxyanisole has been recommended as a temperature calibration material on cooling [18–20]. The published peak onset temperatures show a nearly perfect linear dependence on the heating and cooling rates, each exhibiting the same slope and virtually no step at zero heating rate (cf. Fig. 2).

This behaviour is somewhat unexpected, as this transition is obviously of first order and—at least to some extent—supercooling should occur. Supercooling is a consequence of nucleation phenomena, which occur when the newly emerging

---

[*] Corresponding author. Tel.: +49 531 592 3310; fax: +49 531 592 3305.
E-mail address: stefan.sarge@ptb.de (S.M. Sarge).

0040-6031/$ – see front matter © 2006 Elsevier B.V. All rights reserved.
doi:10.1016/j.tca.2006.03.015

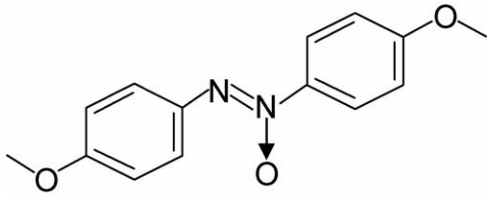

Fig. 1. Structural formula of 4,4′-azoxyanisole (PAA).

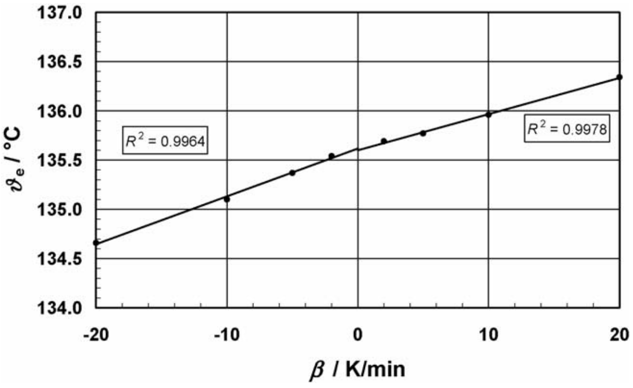

Fig. 2. Dependence of the measured peak onset temperature ϑ_e of the nematic-to-isotropic phase transition of PAA on heating rate β as published in [19,20]. The straight lines are fitted to the measured data points, R^2 gives the coefficient of regression.

phase has little or no structural relation to the parent phase. From light scattering experiments it has been concluded that any isotropic liquid → nematic transition can be supercooled to approximately 1 K at the most [15, pp. 80–81].

2. Purpose of the study

Due to the contradiction between the experimental findings of [12] with respect to the nature of the phase transition and the thermodynamic arguments of [11], a study was undertaken to confirm the suitability of 4,4′-azoxyanisole for temperature calibration of DSCs on cooling as proposed by [19,20].

3. Experimental

The measurements were performed with two differential scanning calorimeters (DSCs) of different designs. One calorimeter was of the power-compensating type (Perkin-Elmer DSC-2, Norwalk, CT, USA, equipped with an instrument control, data acquisition and evaluation unit from IFA GmbH, Ulm, Germany). The temperature of the surroundings was kept at −50 °C by means of the standard liquid nitrogen evaporation cryostat. Argon was used as purge gas. The other calorimeter was a heat flow calorimeter with disk-type measuring system (Mettler Toledo DSC822^e, Star^e-Software, V. 6.10, Greifensee, Switzerland), equipped with the standard cooling unit and purged with nitrogen. All measurements were performed in standard aluminium crucibles. The calorimeters were not explicitly calibrated with respect to their temperature or heat flow rate scales, so the given temperatures can only be used for comparison within one experimental series.

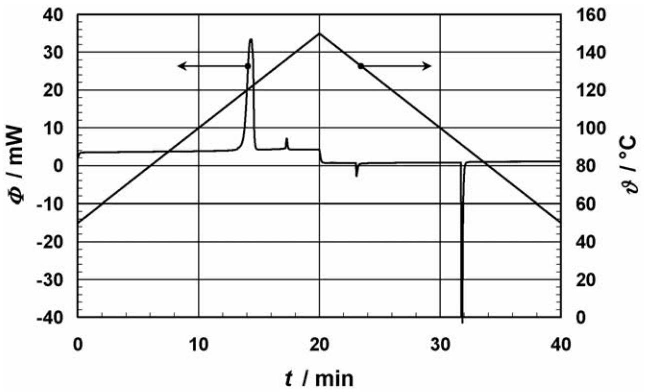

Fig. 3. Typical heating and cooling run at a heating rate $\beta = \pm 5$ K/min of a sample of 4,4′-azoxyanisole with mass $m = 9.582$ mg. The left axis shows the measured heat flow rate Φ, the right axis the temperature ϑ, the abscissa is the time t. The large peaks refer to the transitions from the crystalline to the nematic phase and vice versa, the small peaks refer to the transitions from the nematic phase to the isotropic liquid phase and vice versa.

In all experiments, 4,4′-azoxyanisole (in the following abbreviated as PAA) from Fluka, Buchs, Switzerland, with a stated purity of greater than 98% was used without further purification.

In total, five measurement series were performed. Each series consisted of a number of heating runs at different heating rates, each one immediately followed by a cooling run at the corresponding cooling rate. The heating rates β were varied between ±0.5 and ±20 K/min. The sample mass m was between approximately 5 and 20 mg.

Fig. 3 shows the measured heat flow rate Φ and the temperature ϑ as a function of time t for a typical experiment, here performed with a sample mass $m = 9.582$ mg at a heating rate $\beta = \pm 5$ K/min with the Perkin-Elmer DSC. The transition from the crystalline to the liquid-crystalline nematic phase is connected with a large change in enthalpy. The transition from the nematic to the isotropic liquid phase has a comparably small enthalpy change.

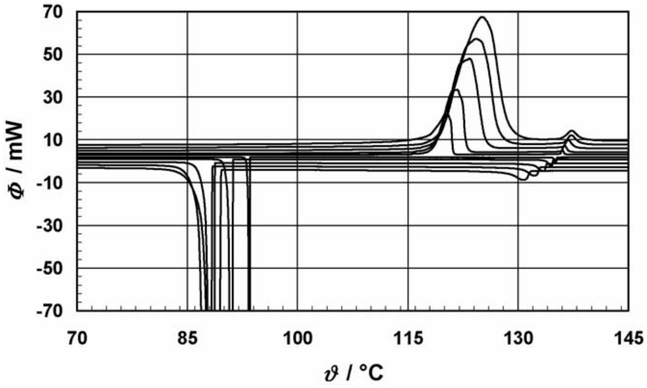

Fig. 4. Series of measurements with the Perkin-Elmer DSC on a sample with mass $m = 9.582$ mg. The upper five curves relate to heating. From upper to lower curves: heating rates $\beta = 20$, 15, 10, 5 and 2 K/min. The lower five curves relate to cooling. From lower to upper curves: cooling rates $\beta = 20$, 15, 10, 5 and 2 K/min. Φ, measured heat flow rate; ϑ, temperature.

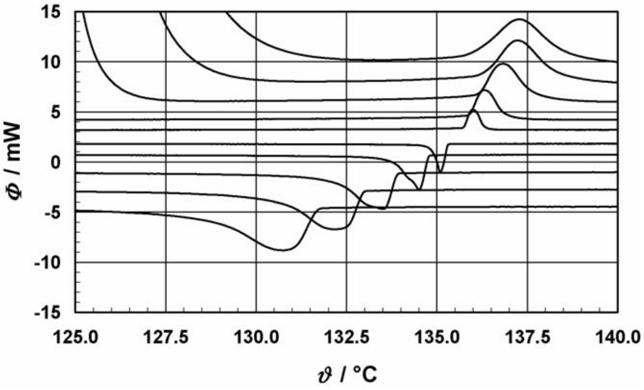

Fig. 5. Same as Fig. 4, enlarged to show the nematic ↔ isotropic liquid transition only.

The results of one measurement series are shown in Fig. 4, where a sample with mass $m = 9.582$ mg was measured at heating rates $\beta = \pm 2$, ± 5, ± 10, ± 15 and ± 20 K/min. The shift of the transition temperatures with changing heating rates can be clearly seen on the crystalline-to-nematic and nematic-to-isotropic liquid phase transition on heating and on the isotropic liquid-to-nematic phase transition on cooling. The nematic-to-crystalline phase transition supercools considerably. As a consequence, when the transition takes place, the crystallization enthalpy is suddenly released and leads to saturation of the power amplifier of the calorimeter. Fig. 5 gives an enlarged picture of Fig. 4 focused on the nematic-to-isotropic liquid (and vice versa) phase transitions. Because of the large peak of the crystalline-to-nematic phase transition it has been recommended [19] to perform calibration experiments focused on the nematic-to-isotropic liquid transition in such a way that the sample is only cooled down to a temperature where this transition, which readily supercools, does not yet occur (minimum 100 °C).

As characteristic temperature of the peak, the peak onset temperature is used. This temperature is defined as the intersection of the extrapolated initial baseline before the peak with the leading edge of the peak. Because of a large pre-transition effect, this is not advisable here. Instead, the intersection of the leading edge of the peak with the interpolated baseline has been used.

When performing the experiments, all runs of a series were performed immediately one after the other without removing the sample from the calorimeter.

4. Results

As already mentioned, five measurements series were carried out. In Table 1, all results have been compiled. Straight lines have been independently fitted to the data from each heating and cooling run. The characteristics of these straight lines, the slope $d\vartheta_e/d\beta$, the intercept $\vartheta_e(\beta = 0)$, and the coefficient of regression R^2 are given, together with the calculated step in ϑ_e of each series of experiments at zero heating rate $\Delta T_e(\beta = 0)$.

Figs. 6 and 7 show the results obtained during this study and, for comparison, those from the literature [19,20].

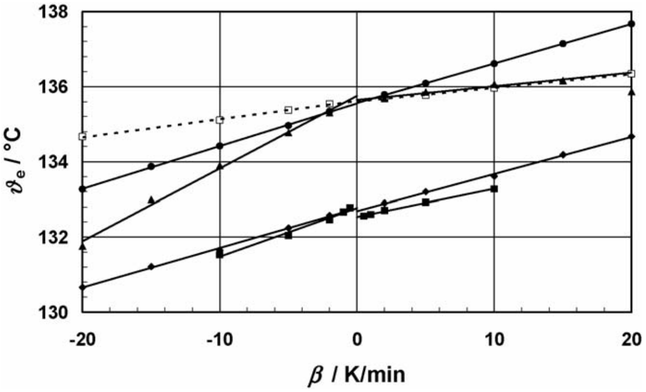

Fig. 6. Extrapolated peak onset temperatures ϑ_e for the nematic-to-isotropic liquid phase transition of 4,4′-azoxyanisole at different heating and cooling rates β. The straight lines are independently fitted to the measured temperatures for heating and for cooling. Each symbol represents one experiment. Open squares and dotted lines: Instrument: Rheometric Scientific DSC-GOLD, sample mass $m = 25.10$ mg, data from [19,20]. Solid lines: Instrument: Perkin-Elmer DSC-2; circles and triangles: $m = 9.582$ mg; diamonds: $m = 2.981$ mg; squares: $m = 17.789$ mg. The shift of approximately 3 K between the lines is due to different calibrations of the calorimeters.

5. Discussion

Our results and those from the literature [11,15] show that the nematic-to-isotropic liquid transition of 4,4′-azoxyanisole is not a phase transition of purely first order but a so called weakly first order transition with a specific transition enthalpy Δh_{trs} of approximately 3 J/g. The experiments show that there is nearly a linear dependence in the peak onset temperatures on higher heating and cooling rates, respectively, as can be inferred from the coefficients of regression R^2 from Table 1. The step at zero heating rate is almost negligibly small. However, the slopes of the two straight lines differ from experiment to experiment.

Fig. 8 shows the peak forms of the nematic ↔ isotropic liquid transition. It is obvious from the large “pre-transition” during heating and the shoulder on the cooling peak that the phase

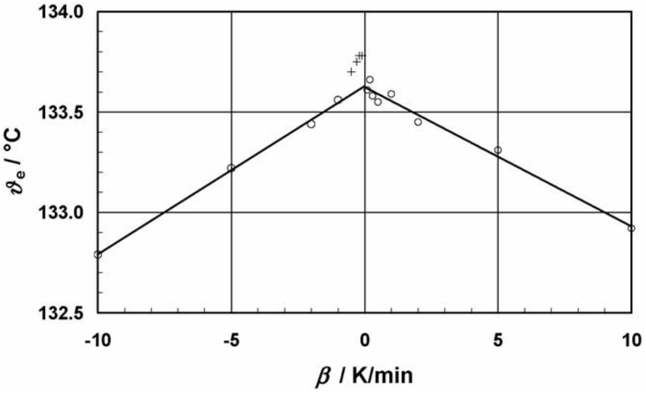

Fig. 7. Extrapolated peak onset temperatures ϑ_e for the nematic-to-isotropic liquid phase transition of 4,4′-azoxyanisole at different heating and cooling rates β. The straight lines are independently fitted to the measured temperatures for heating and for cooling. Each symbol represents one experiment. Instrument: Mettler DSC822^e, sample mass $m = 4.944$ mg, the data at $\beta = \pm 20$ K/min and -0.5 K/min $\leq \beta \leq -0.1$ K/min (crosses) have been excluded from the fitting process.

Table 1
Compilation of measurement results, own and from literature [19,20], and calculated properties of the data from the fitted straight lines, for the nematic-to-isotropic liquid phase transition of 4,4′-azoxyanisole

	Instrument					
	Rheometric Scientific DSC-GOLD [19,20]	Perkin-Elmer DSC-2/IFA				Mettler Toledo DSC822[e]
m/mg	25.10	2.918	9.582	9.582	17.789	4.944
β/K/min	ϑ_e/°C	ϑ_e/°C	ϑ_e/°C	ϑ_e/°C	ϑ_e/°C	ϑ_e/°C
−20	134.66	130.665	131.759	133.269		132.32
−15		131.213	132.993	133.868		
−10	135.10	131.649	133.891	134.414	131.524	132.79
−5	135.37	132.240	134.770	134.957	132.041	133.22
−2	135.54	132.574	135.304	135.338	132.458	133.44
−1					132.662	133.56
−0.5					132.773	133.70
−0.3						133.75
−0.2						133.78
−0.1						133.81
$\mathrm{d}T_e/\mathrm{d}\beta$/s	2.9	6.3	11.6	6.8	7.8	5.0[a]
$\vartheta_e(\beta = 0)$/°C	135.617	132.762	135.754	135.550	132.770	133.629
R^2	0.996	0.998	0.994	0.999	0.984	0.998
β/K/min	ϑ_e/°C	ϑ_e/°C	ϑ_e/°C	ϑ_e/°C	ϑ_e/°C	ϑ_e/°C
0.1						133.61
0.2						133.66
0.3						133.58
0.5					132.556	133.55
1					132.600	133.59
2	135.69	132.897	135.680	135.784	132.702	133.45
5	135.77	133.199	135.852	136.081	132.925	133.31
10	135.96	133.616	136.058	136.611	133.274	132.92
15		134.184	136.155	137.140		
20	136.34	134.669	135.866	137.671		132.66
$\mathrm{d}T_e/\mathrm{d}\beta$/s	2.2	5.9	2.2[b]	6.3	4.5	−4.2[b]
$\vartheta_e(\beta = 0)$/°C	135.601	132.688	135.645	135.564	132.534	133.624
R^2	0.998	0.998	0.958	1.000	0.997	0.980
$\Delta T_e(\beta = 0)$/K	−0.016	−0.074	−0.109	0.014	−0.236	−0.005

[a] This fitting process has been performed for the data points of $-10\,\mathrm{K/min} \leq \beta \leq -1\,\mathrm{K/min}$ only.

[b] This fitting process has been performed for the data points of $\beta \leq 10\,\mathrm{K/min}$ only.

transition is not of simple first order but obviously more complex. This effect has been exploited for the determination of the resolution of DSCs [10] and results in additional uncertainties with respect to the construction of the baselines and, as a consequence, in the calculation of the extrapolated peak onset temperatures. This uncertainty amounts to several tenths of a degree and is only avoided here because the data have been evaluated by one person applying always the same evaluation pattern. Automatic routines for the determination of the extrapolated peak onset temperature often fail because of the pre-transition phenomenon. Furthermore, the very steep slope of the exothermic peak on cooling indicates that the total enthalpy of transition is released in one instant when after supercooling of the sample, especially at low cooling rates, nucleation occurs.

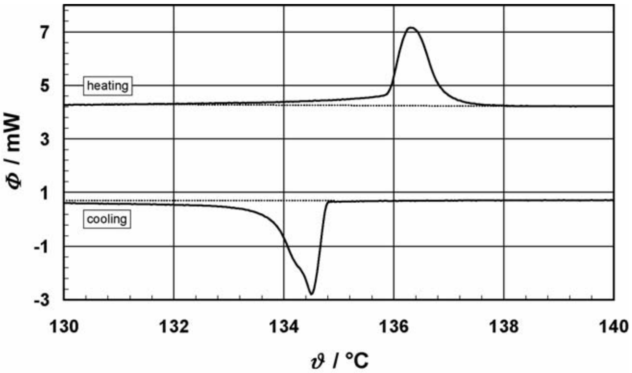

Fig. 8. Heating and cooling peak at a medium rate ($\beta = \pm 5\,\mathrm{K/min}$) of the nematic ↔ isotropic liquid transition of 4,4′-azoxyanisole. The dotted lines represent linearly interpolated baselines under the peaks. Φ, measured heat flow rate; ϑ, temperature.

The dependence of the extrapolated peak onset temperatures on the heating rate for the Mettler DSC is unexpected but may be explained with the calibration algorithms in the evaluation software. Mettler Toledo uses a procedure to correct the measured temperatures for the heating rate effect. This procedure requires information about the magnitude of this effect, which is exactly the figure we were trying to determine by experiment in this study. If this parameter overestimates the heating rate effect, an inverse dependence may result. This correction factor, called τ_{lag}, is described in the software by a linear equation with temperature as the parameter. At $\vartheta = 130\,°\mathrm{C}$, $\tau_{\mathrm{lag}} = 2.3\,\mathrm{s}$ is valid. Surprisingly, the evaluation software does not apply this correction to measurements performed in the cooling mode.

Another, even more worrying argument has been put forward by Wunderlich and co-workers [21,22]. They calibrated DSCs of three different manufacturers with indium and PAA at different heating and cooling rates between ±20 and ±0.2 K/min and observed at sigmoidal shape of the dependence of the extrapolated peak onset temperatures on the heating rate β between approximately -0.5 and $+0.5$ K/min. At higher heating and cooling rates the dependence became linear. He attributed this effect to an instrumental artefact, i.e. that at low heating or cooling rates the latent heat of transition keeps the sample temperature and, thus, the sensor temperature constant. When then the temperature controller of the furnace tries to keep the heating rate constant, an additional heat input (on heating) or heat subtraction (on cooling) is necessary. This additional heat causes a deviation from the programmed heating rate, thus pretending a non-linear behaviour of the system. The same effect has been observed in our experiments with the Mettler Toledo DSC (cf. Fig. 7). However, Wunderlich's argumentation only holds for instruments where the temperature controller is influenced by the temperature sensor underneath the sample crucible or even uses this sensor for control purposes. This is definitely true for the Perkin-Elmer power compensation DSCs but is unknown—at least to the authors of this paper—for modern heat flow DSCs like TA Instrument's or Mettler Toledo's DSCs. Furthermore, the published data are symmetric around $\beta = 0$. This is strange, because the temperature of the sample during the phase transition is different in heating and in cooling: in heating, the temperature of the sample remains constant during the transition process until all the material is isotropic, whereas in cooling, the temperature of the sample increases from the supercooled state to the equilibrium transition temperature as soon as nucleation has occurred.

6. Conclusions

The nematic to isotropic liquid transition of 4,4′-azoxyanisole is a phase transition of weakly first order with pre-transition effect the physical meaning of which is still unknown. Consequently, it should be used for calibration in the cooling mode with due care. Additionally, the theory behind the operation of DSCs seems more complex than often anticipated and, obviously, still deserves further elucidation. The same applies to the evaluation algorithms and procedures hidden in the software of the manufacturers of the calorimeters.

Acknowledgements

The authors gratefully acknowledge the many extended, encouraging and fruitful discussions with Walter Eysel†, Eberhard Gmelin, Wolfgang Hemminger, and Günther W.H. Höhne.

References

[1] J.D. Menczel, T.M. Leslie, Thermochim. Acta 166 (1990) 309–317.
[2] J.D. Menczel, T.M. Leslie, J. Thermal Anal. 40 (1993) 957–970.
[3] J.D. Menczel, J. Thermal Anal. 49 (1997) 193–199.
[4] C. Schick, G.W.H. Höhne, Thermochim. Acta 187 (1991) 351–356.
[5] G.W.H. Höhne, J. Schawe, C. Schnick, Thermochim. Acta 221 (1993) 129–137.
[6] J.A. Martins, J.J.C. Cruz-Pinto, Thermochim. Acta 332 (1999) 179–188.
[7] M.J.A. Malheiro, J.A. Martins, J.J.C. Cruz Pinto, Thermochim. Acta 420 (2004) 155–161.
[8] S.M. Sarge, G.W.H. Höhne, H.K. Cammenga, W. Eysel, E. Gmelin, Thermochim. Acta 361 (2000) 1–20.
[9] Z. Bashir, N. Khan, D.M. Price, Thermochim. Acta 319 (1998) 47–53.
[10] P.J. van Ekeren, C.M. Holl, A.J. Witteveen, J. Thermal Anal. 49 (1997) 1105–1114.
[11] R. Alben, Mol. Cryst. Liq. Cryst. 10 (1970) 21–29.
[12] P. Narvard, J.M. Haudin, J. Thermal Anal. 30 (1985) 61–64.
[13] P. Narvard, J.M. Haudin, J. Thermal Anal. 29 (1984) 408–414.
[14] P. Narvard, J.M. Haudin, J. Thermal Anal. 29 (1984) 415–421.
[15] P.G. de Gennes, J. Prost, The Physics of Liquid Crystals, 2nd ed., Clarendon Press, Oxford, 1993.
[16] N.M. Sakevich, Isv. Vuz. Fiz. 10 (1967) 52–56.
[17] H. Kelker, R. Hatz, Handbook of Liquid Crystals, Verlag Chemie, Weinheim, 1980, pp. 340–383.
[18] G. Hakvoort, C.M. Hol, J. Thermal Anal. 52 (1998) 195–202.
[19] G. Hakvoort, C.M. Hol, J. Thermal Anal. Calorim. 56 (1999) 717–722.
[20] G. Hakvoort, C.M. Hol, P.J. van Ekeren, J. Thermal Anal. Calorim. 64 (2001) 367–375.
[21] K. Ishikiriyama, A. Boller, B. Wunderlich, J. Thermal Anal. 50 (1997) 547–558.
[22] W. Chen, M. Dadnum, Z. Zhang, A. Boller, B. Wunderlich, Thermochim. Acta 324 (1998) 87–94.